Supporting Information

Thiennimitr et al. 10.1073/pnas.1107857108

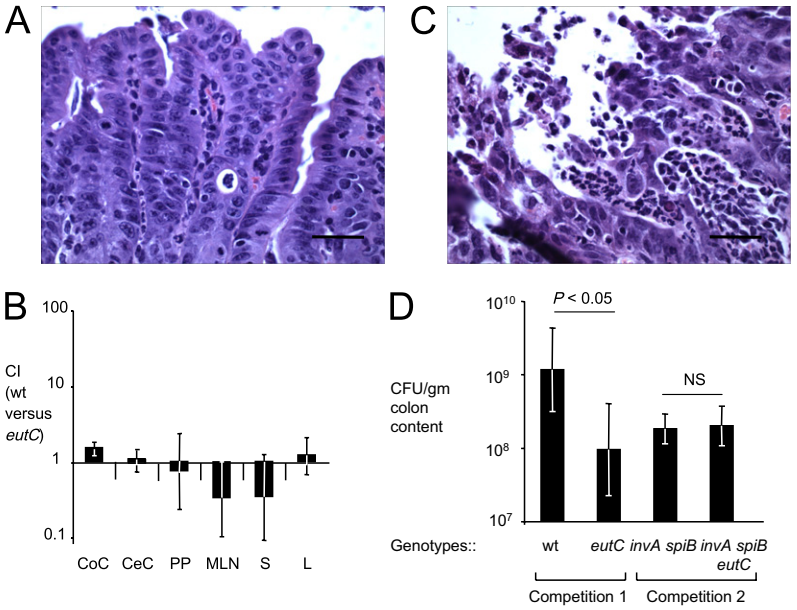

Fig. S1. Contribution of ethanolamine utilization to colonization in the typhoid mouse model versus the mouse colitis model. (*A*) Representative image (80×) of H&E-stained cecal sections from the mouse typhoid model. Note the predominant monocytic infiltrate. (Scale bar, 50 μm.) (*B*) Mice (mouse typhoid model) were orally inoculated with an equal mixture of the *Salmonella enterica* serovar Typhimurium (*S.* Typhimurium) wild-type (wt) *eutC* mutant (PT100). Four days after infection, bacteria were recovered from the tissues, as indicated, and the competitive index (CI) calculated. CoC, colon content; CeC cecal content; PP, Peyer's patches; MNL, mesenteric lymph node; S, spleen; L, liver. (*C*) Representative image (80×) of H&E-stained cecal sections from the mouse colitis model. Note the exudative inflammation and concomitant neutrophilic infiltration. (Scale bar, 50 μm.) (*D*) Mice (mouse colitis model) were orally inoculated with an equal mixture of the *S.* Typhimurium wild-type (wt) and the *eutC* mutant (PT100) (competition 1) or an *invA spiB* mutant and a *invA spiB eutC* mutant (competition 2). Data represent the geometric mean from four animals ± SE.

A

Score	Neutrophil infiltration*	Mononuclear leukocyte infiltration*	Submucosal edema	Epithelial damage	Exudate
0	No changes (0-5)	No changes (0-5)	No changes	No changes	No changes
1	6-20	5-10	Detectable (<10%)	Desquamation	Slight accumulation
2	21-60	10-20	Mild (10-20%)	Mild erosion and mild loss of goblet cells/ undifferentiated enterocytes hyperplasia	Mild accumulation
3	61-100	20-40	Moderate (20-40%)	Marked erosion and moderate loss of goblet cells/ undifferentiated hyperplasia	Moderate accumulation
4	>100	>40	Marked (>40%)	Ulceration and marked loss of goblet cells/ undifferentiated hyperplasia	Marked accumulation

*Number of cells per high power field (400X)

B

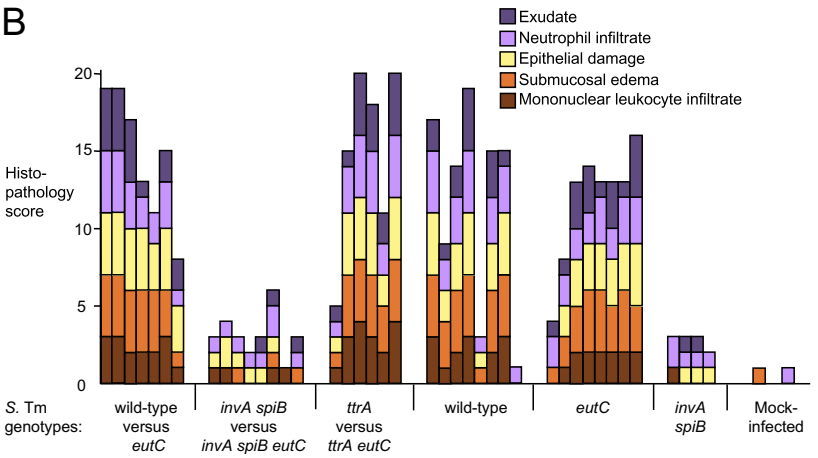

Fig. S2. Analysis of cecal inflammation in the mouse model of *Salmonella*-induced colitis. (*A*) Chart listing criteria for the scoring of H&E-stained cecal sections. (*B*) Detailed representation of the histopathological scoring for each individual animal shown in Figs. 2*A* and 4*A*. For data shown in the three panels to the left, mice were inoculated with mixtures of the following strains: wild-type (IR715) vs. *eutC* mutant (PT100); *invA spiB* mutant (SPN452) vs. *invA spiB eutC* mutant (PT102); or *ttrA* mutant (SW661) vs. *ttrA eutC* mutant (PT106).

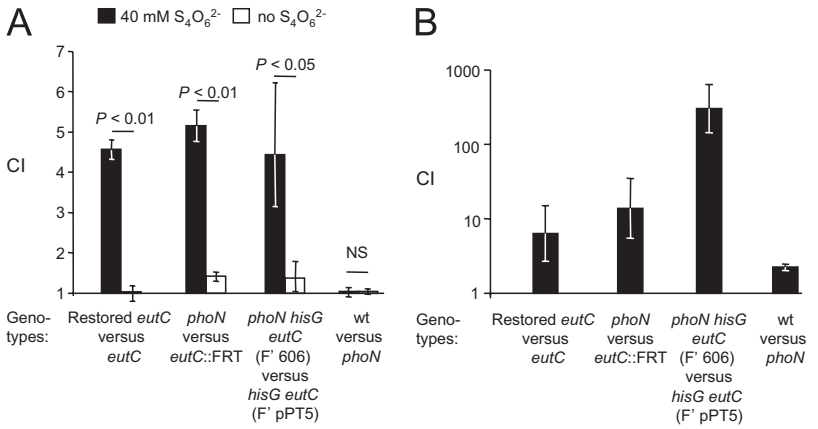

Fig. S3. The *eut* gene cluster confers a growth advantage during anaerobic growth in ethanolamine broth (*A*) and in the mouse colitis model (*B*). (*A*) Competitive indices of the following *S.* Typhimurium strains are shown (from left to right): restored *eutC* (PT238) vs. *eutC* mutant (PT100); *phoN* mutant (AJB715) vs. Δ*eutC*::FRT mutant (TT26355); *phoN hisG eutC* (F′ 606) mutant (PT251) vs. *hisG eutC* (F′ pPT5) mutant (TT26358); wild-type (IR715) vs. *phoN* mutant (AJB715). Bacterial numbers were determined 24 h after anaerobic growth with ethanolamine as the sole carbon source in the presence (black bars) or absence (white bars) of tetrathionate ($S_4O_6^{2-}$). Data represent the geometric mean ± SE. (*B*) Competitive indices of *S.* Typhimurium strains recovered from the colon content of streptomycin-pretreated mice (C57BL/6) 4 d after infection (mouse colitis model).

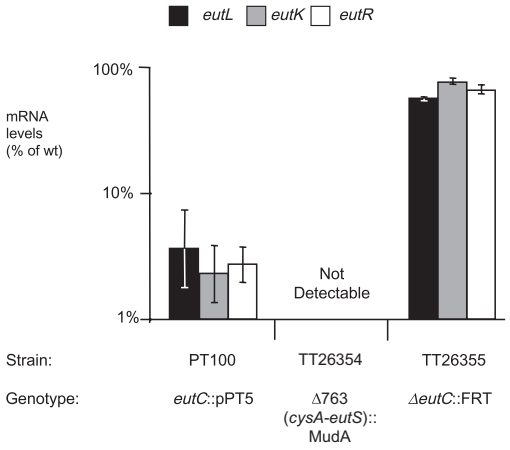

Fig. S4. Polarity of *eutC*::pPT5 and Δ*eutC*::FRT mutations on expression of downstream genes. Expression levels of the *eutLKR* genes, which are located downstream of the *eutC* gene, were determined by quantitative real-time PCR with primers listed in Table S2. Each experiment was repeated three times independently. Data represent geometric mean ± SE of mRNA levels detected for *eutL* (black bars), *eutK* (gray bars), and *eutR* (open bars) relative to mRNA levels detected for these genes in the *S*. Typhimurium wild-type strain (IR715), which were set to 100%. A strain lacking the entire *eut* operon (TT26354) was used as a negative control.

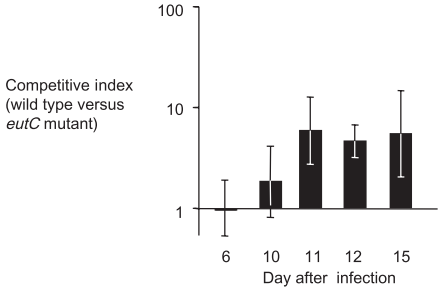

Fig. S5. Ethanolamine utilization genes confer a growth advantage in streptomycin-pretreated genetically resistant (129/svJ) mice. Competitive indices of *S*. Typhimurium strains recovered from the fecal pellets (days 6–12) and colon contents (day 15). Data represent the geometric mean ± SE.

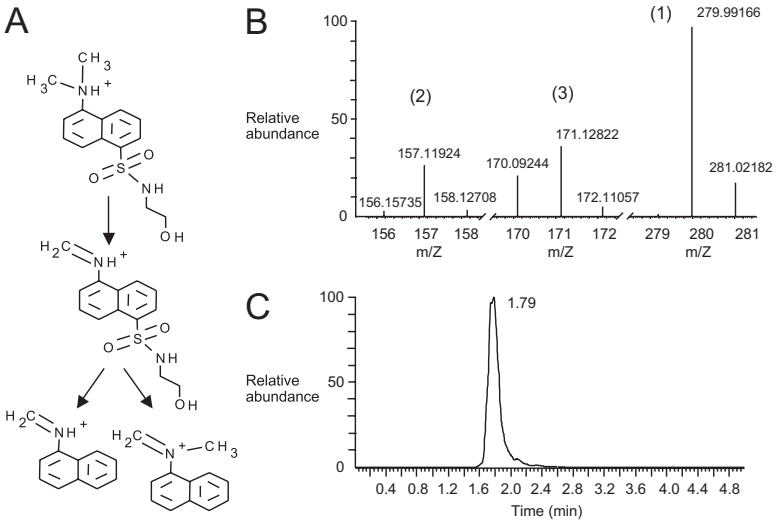

Fig. S6. Quantification of ethanolamine in colonic extracts by LC-MS/MS. (*A*) Structural formula of fragments of derivatized ethanolamine ([*N*-dansyl]ethanolamine). (*B*) Representative single-ion monitoring scan spectra of the parent ions depicted in *A*. (*C*) Representative elution profile of transition 295/280; [*N*-dansyl]ethanolamine breakdown product.

Table S1. Bacterial strains and plasmids used in this study

Designation	Genotype and relevant characteristics	Reference
S. typhimurium strains		
IR715	Nalidixic acid-resistant derivative of ATCC 14028	(1)
SPN452	IR715 Δ*invA*::*tetRA* Δ*spiB*::KSAC	(2)
SW661	IR715 *ttrA*::pSW171	(3)
PT100	IR715 *eutC*::pPT5	Present study
AJB715	IR715 *phoN*::KSAC	(4)
PT102	IR715 Δ*invA*::*tetRA* Δ*spiB*::KSAC *eutC*::pPT5	Present study
PT106	IR715 *ttrA*::pSW171 *eutC*::pPT5	Present study
TT26354	IR715 Δ763(*cysA-eutS*)::MudA	(5)
PT238	PT100 *eutC* restored	Present study
TT26355	IR715 Δ*eutC*::FRT	(6)
TT26356	IR715 *hisG*::Tn*10*d-Tet *eutC*::pPT5 (F′ 606)	Present study
PT251	IR715 *hisG*::Tn*10*d-Tet *phoN*::KSAC *eutC*::pPT5 (F′ 606)	Present study
TT26358	IR715 *hisG*::Tn*10*d-Tet *eutC*::pPT5 (F′ pPT5)	Present study
Plasmids		
pCR2.1	Cloning vector	Invitrogen
pEP185.2	*ori*(R6K) *mobRP4 cat*	(7)
pPT3	‘*eutC*’ cloned into pCR2.1	Present study
pPT5	‘*eutC*’ cloned into pEP185.2	Present study
F′ 606	F plasmid carrying *his* locus and *eut* locus	(8)
F′ pPT5	F′ 606 *eutC*::pPT5	Present study

1. Stojiljkovic I, Bäumler AJ, Heffron F (1995) Ethanolamine utilization in *Salmonella typhimurium*: Nucleotide sequence, protein expression, and mutational analysis of the *cchA cchB eutE eutJ eutG eutH* gene cluster. *J Bacteriol* 177:1357–1366.
2. Raffatellu M, et al. (2009) Lipocalin-2 resistance confers an advantage to *Salmonella enterica* serotype typhimurium for growth and survival in the inflamed intestine. *Cell Host Microbe* 5:476–486.
3. Winter SE, et al. (2010) Gut inflammation provides a respiratory electron acceptor for *Salmonella*. *Nature* 467:426–429.
4. Kingsley RA, et al. (2003) Molecular and phenotypic analysis of the CS54 island of *Salmonella enterica* serotype typhimurium: Identification of intestinal colonization and persistence determinants. *Infect Immun* 71:629–640.
5. Kofoid E, Rappleye C, Stojiljkovic I, Roth J (1999) The 17-gene ethanolamine (eut) operon of *Salmonella typhimurium* encodes five homologues of carboxysome shell proteins. *J Bacteriol* 181:5317–5329.
6. Penrod JT, Roth JR (2006) Conserving a volatile metabolite: A role for carboxysome-like organelles in *Salmonella enterica*. *J Bacteriol* 188:2865–2874.
7. Kinder SA, Badger JL, Bryant GO, Pepe JC, Miller VL (1993) Cloning of the YenI restriction endonuclease and methyltransferase from *Yersinia enterocolitica* serotype O8 and construction of a transformable R-M+ mutant. *Gene* 136:271–275.
8. Roof DM, Roth JR (1992) Autogenous regulation of ethanolamine utilization by a transcriptional activator of the eut operon in *Salmonella typhimurium*. *J Bacteriol* 174:6634–6643.

Table S2. Primers used in this study

Organism	Target gene/purpose	Sequence
Mus musculus	*Gapdh*/qRT-PCR	5′-TGTAGACCATGTAGTTGAGGTCA-3′
		5′-AGGTCGGTGTGAACGGATTTG-3′
M. musculus	*Kc*/qRT-PCR	5′-TGCACCCAAACCGAAGTCAT-3′
		5′-TTGTCAGAAGCCAGCGTTCAC-3′
M. musculus	*Nos2*/qRT-PCR	5′-TTGGGTCTTGTTCACTCCACGG-3′
		5′-CCTCTTTCAGGTCACTTTGGTAGG-3′
S. Typhimurium	*gmk*/qRT-PCR	5′-TTGGCAGGGAGGCGTTT-3′
		5′-GCGCGAAGTGCCGTAGTAAT-3′
S. Typhimurium	*eutL*/qRT-PCR	5′-GCGACAAAACAGGCGATGG-3′
		5′-ACACCTCACCAGCGGTAGG-3′
S. Typhimurium	*eutK*/qRT-PCR	5′-GAAGTGGACGGAATGGTCG-3′
		5′-GATGACTGAGCAAACGCACG-3′
S. Typhimurium	*eutR*/qRT-PCR	5′-TGGACAATGTTCATCAGCGAC-3′
		5′-CATCAAGCAGGATTTCCGTG-3′
S. Typhimurium	*eutC*/insertional inactivation of *eutC*	5′-GAGCTCTTGTACGTAGCGTGATG-3′
		5′-GGTACCGCACTGTGACTTCAG-3′